BIW10 Preprint -- Edited; preliminary green dot status
Final version will appear on JACoW

OTR POLARIZATION EFFECTS IN BEAM-PROFILE MONITORS AT THE FERMILAB A0 PHOTOINJECTOR*

A. Lumpkin#, A. Johnson, J. Ruan, J. Santucci, and R.Thurman-Keup
Fermilab, Batavia, IL U.S.A. 60510

Abstract

Optical transition radiation (OTR) imaging for transverse beam-size characterization is a well-established technique at many accelerators including the Fermilab A0 photoinjector (A0PI) facility. With low beam energies of 14-15 MeV and emittances of 3 mm mrad, one observes beam sizes of 0.8 to 1.5 mm (sigma). However, the use of 50-μm wide slits to sample the beam's transverse phase spaces significantly alters the required resolution of the converter screen and imaging system. Slit-image sizes of about sigma =100 μm or less are observed, depending on drift distance and beam divergence. Moreover, the OTR polarized component perpendicular to the narrow beam dimension systematically gave us ~20-μm smaller projected image sizes than those with the total OTR intensity. This is one of the first reports of this polarization effect at such a low-gamma regime (~30).

INTRODUCTION

The opportunity for a new series of beam characterization experiments at the Fermilab A0 photoinjector (A0PI) was recognized in the last year. There is an ongoing proof-of-principle experiment to demonstrate the exchange of the transverse horizontal and longitudinal emittances [1,2]. This experiment relies on measurements of the transverse emittances and longitudinal emittance upstream and downstream of an emittance-exchange (EEX) beamline. Generally, at the low beam energies of 14-15 MeV and emittances of 3-5 mm mrad, one encounters beam sizes of 0.8 to 1.5 mm (sigma) [2]. Such beam sizes do not present a challenge to standard imaging procedures using scintillator screens or optical transition radiation (OTR) screens as described elsewhere [3]. However, the slits-emittance-measurement technique [4] which involves insertion of 50-μm wide slits to sample the beam's transverse phase spaces significantly alters the required resolution of the converter screen and imaging system. In this case, one deals with slit-image sizes of σ =100 μm or less, and depending on the drift distance one deals with images that can approach the camera resolution limit and/or the converter screen resolution limit. Beam divergence is calculated from the downstream slit image size and the relevant drift distance.

*Work supported by U.S. Department of Energy, Office of Science, Office of High Energy Physics, under Contract No. DE-AC02-07CH1135.
#lumpkin@fnal.gov

In the case of OTR imaging for transverse beam-size characterization, there is empirical evidence for gamma greater than 1000 beams that the utilization of the polarization component orthogonal to the dimension of interest results in a smaller projected image profile [5-7]. This aspect is a small fractional correction for 1-mm sized beam spots, but quite noticeable for 150-μm sized beam spots. While evaluating the slit images for emittance measurements at A0PI, we consistently found that using the OTR polarized component orthogonal to the narrow beam dimension of interest systematically gave us ~20 μm smaller projected image sizes than with the total OTR intensity. For such a low-gamma regime (~30), this is one of the first reports of this polarization effect on observed beam sizes. This correction affects the emittance values through the beam-size-divergence product.

EXPERIMENTAL BACKGROUND

The tests were performed at the Fermilab A0 photoinjector facility which includes an L-band photocathode (PC) rf gun and a 9-cell superconducting radiofrequency (SCRF) accelerating structure which combine to generate up to 16-MeV electron beams [2]. The drive laser operates at 81.25 MHz although the micropulse structure is usually counted down to 1 MHz. Due to the low, electron-beam energies and OTR signals, we typically summed over 50 micropulses with 0.25 nC per micropulse. The tests were performed in the straight-ahead line where energizing a dipole sends the beam into a final beam dump. The setup included the upstream corrector magnets, quadrupoles, the YAG:Ce and/or OTR imaging stations denoted as X3-X6, and the beam dump as schematically shown in Fig. 1. Both the YAG:Ce powder screen and the OTR screens were oriented with the surface normal at 45 degrees to the beam direction and with the viewing port at 90 degrees to the beam direction. The OTR converter was an Al-coated optics mirror that was 1.0 mm thick with a BK7 substrate and was mounted on a stepper assembly. The assembly provided vertical positioning with an option for the YAG:Ce scintillator at X5. The images were obtained with a 10-bit Firewire digital CCD camera with an optical transport consisting of a 150-mm-focal-length field lens, mirror, and a 50 mm C-mount lens on the camera. The images were captured with 8-bit resolution under the DOOCS protocol, and images were processed with MATLAB-based tools for Gaussian curve fitting to the projected profiles.

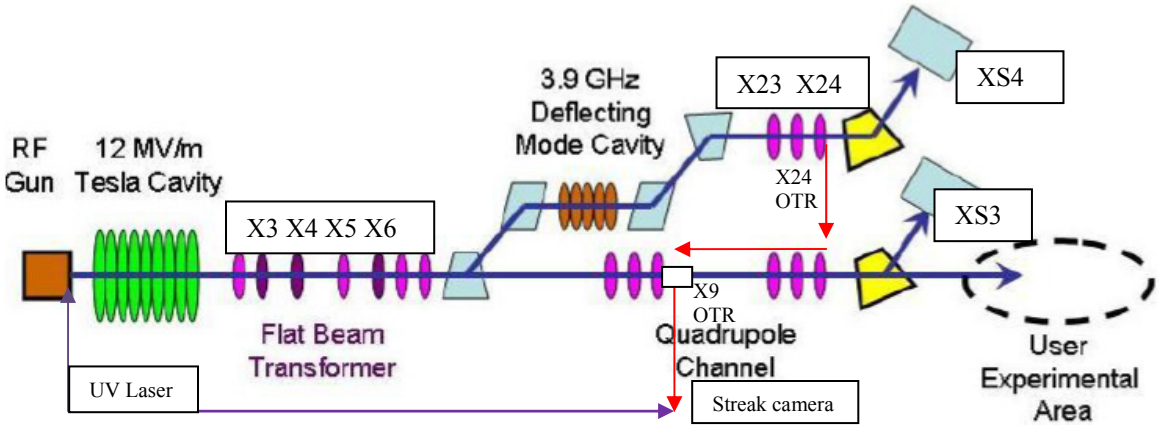

Figure 1: A schematic of the A0 photoinjector test area showing the PC RF gun, 9-cell SCRF Tesla cavity, transverse emittance stations, the OTR stations, and the exchanger beamline when the two doglegs' dipoles are powered.

After inserting the slit assemblies at X3, the initial sampling station was chosen 0.79 m downstream at X5. The slit assemblies were 3 mm thick with the 50-µm wide slits spaced 1 mm apart. The single polarizer was on a pneumatic actuator which allowed for the polarizer to be in the X5 optical path or out of it. The linear polarizer orientation of horizontal or vertical to the beam-direction-observation-direction plane was fixed, and it thus required a tunnel access to rotate manually the polarizer orientation.

OTR POLARIZATION RESULTS

It is well known that OTR is radially polarized, and this leads to a somewhat subtle effect. Some experimental teams have reported a beam-size effect when using a linear polarizer with the OTR. The experiments were performed with much higher gamma beams, such as 56000 at SLAC FFTB [5], 14000 at APS [6], and 9000 at JLAB [7]. In all cases the beam image size was reduced when using the OTR polarization component *orthogonal* to the beam dimension axis. As schematically shown in Fig. 2, the approaching beam charges induce currents in the metal plane that generate the radially polarized OTR. By selecting the vertically polarized component one suppresses the OTR that extends beyond the horizontal charge distribution and obtains a result closer to the actual x beam size.

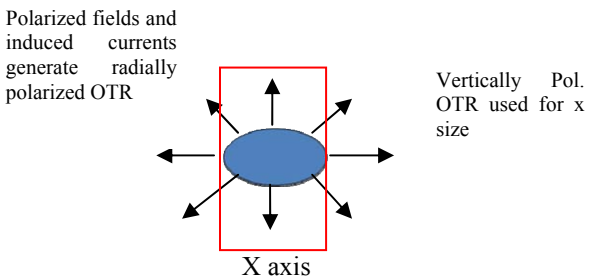

Figure 2: Schematic of the induced currents that generate radially polarized OTR when a charge distribution strikes a metal surface.

In the JLAB case at 4.5 GeV, the observed beam image size was 150 by 161 µm when using the total intensity [7]. With the linear polarizer oriented vertically in the optical path one observed an x image size of 127 µm, while with it oriented horizontally one saw a y image size of 130 µm. The studies of the effects were extended by adjusting an upstream quadrupole's focusing strength to vary the beam size. These were cross checked with results from a nearby wire scanner as shown in Fig. 3. The OTR orthogonally polarized data (black diamonds) systematically fall closer to the wire-scan data (open circles) than the total intensity data.

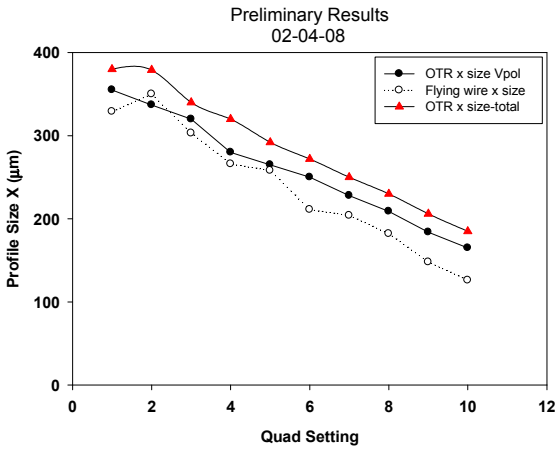

Figure 3: A comparison of the total OTR based beam size, orthogonally polarized OTR based beam size, and the flying wire based beam size for the horizontal dimension [7].

In the A0PI experiments, we systematically observe smaller beam slit images by 10-20 µm with the orthogonally polarized light than with the total OTR for slit images as seen in Fig. 4 and Table I. Since the slit images are in the range of 100 µm, this is an additional size correction. We believe these are the first reports of the effect at such low gamma, although Castellano and Verzilov evaluated a polarization effect at the single-particle-function level and at the few-micron level for a range of beam energies [8].

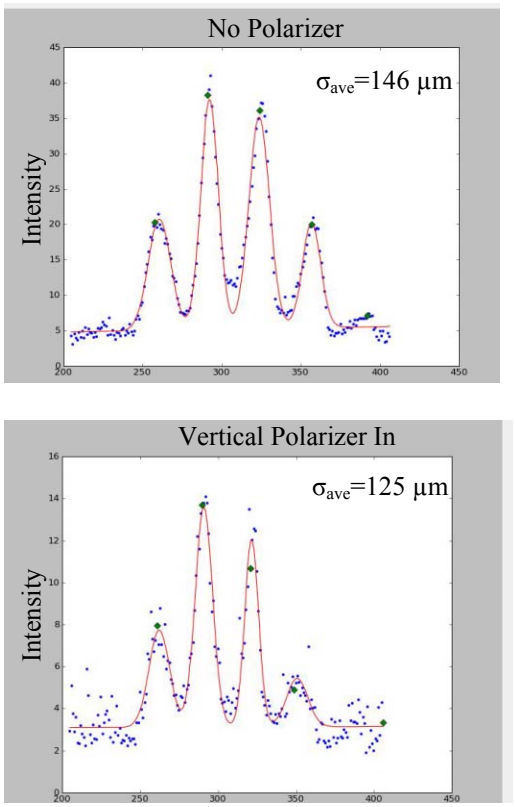

Figure 4: Comparison of X5 vertical slit images without (Upper) and with (lower) the vertical polarizer inserted. The averaged slit image profile width is 0.9 pixels or 20 μm smaller with the vertical polarizer inserted.

Table I: Comparison of OTR beam and slit images at the X5 imaging station using vertical polarization (V). The slits inserted at screen X3 are none (No), horizontal (H), and vertical (V). Five image averages were used for the slit images. (June 18, 2009)

X3 Slit	X5 Pol.	Q (pC)	Bunches	Fit sigma(pix)	Size(μm)
No	No	350	30	x, 38.5	874
No	V	350	30	x, 37.9	860
H	No	350	80	4.3	96.7
H	V	350	80	4.4	99.6
V	No	350	80	5.9	133
V	V	350	80	5.0	114
V	No	1000	80	6.8±0.1	154
V	V	1000	80	5.7 ±0.1	128

We extended these studies by another series of experiments as shown in the following tables. In these case we even checked for effects of the drive laser's S and P polarizations. Data obtained with each are indicated. As can be seen in Table II, the data are organized in columns indicating which slits were inserted at X3, which linear polarizer orientation was used in the optics before the camera at X5, the drive laser polarization, the number of bunches, the image profile fit sigma in pixels, and the size in microns. As stated earlier, the single linear polarizer was on a pneumatic actuator which allowed for the polarizer to be in the optical path or out of it. The linear polarizer orientation of horizontal or vertical to the beam-direction-observation-direction plane was fixed, and it thus required a tunnel access to rotate manually the polarizer. The data are organized in pairs, without and with the polarizer inserted. The projected image profiles in the narrow dimension were fit to a Gaussian shape and the results from ten images were averaged. The average size pixel value and the standard deviation were determined, and then the uncertainty of the mean was calculated by dividing the standard deviation by the square root of the number of samples [9]. This table clearly shows in the first four rows a systematically smaller beam vertical slit image size by 20-21 μm when the vertical polarizer is inserted versus not inserted for either laser polarization. The narrow dimension is actually the horizontal direction in this case. In addition the last four rows show that with horizontal slits inserted at X3, the vertical polarizer has little effect on the parallel vertical dimension size. This configuration should have similar intensities to that of the vertical slits so this check should preclude an intensity-dependent effect in the imaging system for the vertical polarizer data.

Table II: Comparison of slit images using vertically polarized OTR at X5. (July 20, 2009).

X3 Slit	X5 Pol.	Las. Pol.	Bunches	Sigma(pix)	Size(μm)
V	No	S	100	4.04±0.11	91.7
V	V	S	100	3.09±0.08	70.1
V	No	P	100	4.26±0.14	96.7
V	V	P	100	3.37±0.09	76.5
H	No	P	100	4.37±0.07	99.2
H	V	P	100	4.45±0.10	101.0
H	No	S	100	4.34±0.07	98.5
H	V	S	100	4.35 ±0.09	98.7

As a further test, we used an upstream quadrupole's current setting to focus in one plane and form a narrow band at the X5 location. In this case we could approach the size of the slit images, but we had more electrons contributing to the beam image than the slit sample. We actually used ten times fewer bunches for Table III results than in the OTR based slit images of Table II. The same procedure is used as for the slit images, and the vertically polarized data profiles are all smaller by 11-30 μm than the total OTR image for the vertical-band test. When we changed the quadrupole setting to produce a horizontal band with a narrow vertical size at X5, we actually saw a

larger size with the now parallel polarized vertical component.

Table III: Comparison of band images using vertically polarized OTR at X5 and 10 bunches. (July 21, 2009)

X5 Band	X5 Pol.	Las. Pol.	Sigma(pix)	Size (μm)
V	No	P	5.42±0.03	123.0
V	V	P	4.00±0.04	90.8
V	No	S	5.55±0.02	126.0
V	V	S	4.95±0.05	112.4
V	No	P	5.36±0.02	121.7
V	V	P	4.85±0.10	110.1
H	No	P	4.65±0.03	105.5
H	V	P	5.37±0.05	121.9

In the course of the tests, we also obtained data with the YAG:Ce powder screen whose surface normal is oriented at 45 degrees to the beam direction as was the OTR screen. This screen is on the same stepper motor driven actuator as the OTR screen so we could easily select it and use the same X5 optics. The results are shown in Table IV. For comparison purposes we also show the OTR data in the table. First, it is noted that there was evidence for the OTR polarization effect in rows 1,2, and secondly, no polarization effects observed (as expected) in the YAG:Ce-based beam sizes at rows 3,4. Only one bunch was used with the brighter scintillator, so we could be reducing any macropulse effects in the beam. On the average, the vertically polarized OTR band images for the vertical slits in rows 2,6 have a size of 101 μm compared to the total OTR image size of 124.5 μm and to the YAG:Ce averaged image size of 130 μm. These results are consistent with our previous hypothesis that the YAG:Ce powder screen has a limiting resolution term to be addressed [10]. If we accept the OTR polarized data as the reference, then the implied YAG:Ce X5 screen term in quadrature would be 82±9 μm. We understand these have a basic 50-μm thick YAG:Ce deposition on the 1-mm thick Al metal substrate [11].

One of the alternative explanations was that the polarized source was equivalent to a reduction in aperture in the optics, and this could lead to an improved resolution. Figure 5 shows the "polarizer out" minus "polarizer in" sigma vs. lens f/#. The red datum point was obtained with vertical slits and vertical polarizer and the blue data points were from the horizontal slits and horizontal polarizer configuration. The green datum point is calculated from slit images that weren't properly rotated so the projected size was enlarged for the polarized data. The data also reflect an asymmetry in the magnitude of the differences for the vertical and horizontal polarizer data, with the latter having statistically smaller effects by a factor of about two. However, the polarization effect persists at f/#4, albeit with low signals even with the large number of bunches in the macropulse.

Table IV: Comparison of OTR and YAG:Ce powder band images at X5 for 250 pC per bunch. The YAG:Ce powder data used only 1 bunch as denoted by 1-Y in col. 4. (July 21, 2009)

X5 Band	X5 Pol.	Bunches	Fit sigma (pix)	Size (μm)
V	No	10	5.42±0.03	123.0
V	V	10	4.00±0.04	90.8
V	No	1-Y	5.67±0.09	128.7
V	V	1-Y	5.71±0.04	129.6
V	No	10	5.55±0.02	126.0
V	V	10	4.95±0.10	112.4
H	No	1-Y	5.63±0.08	127.8
H	V	1-Y	5.92±0.05	134.4

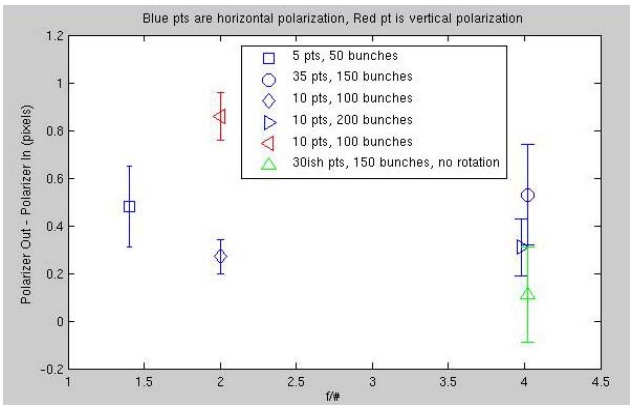

Figure 5: Plot of the "polarizer out" minus "polarizer in" observed beam size difference in pixels (with a calibration factor of 22.8 μm/pixel) versus f/#. The polarized OTR gives systematically smaller beam sizes. (July 2, 2009).

We note that the Al OTR screen is rotated around the vertical axis which fundamentally breaks the symmetry for the two radiation lobes in the horizontal axis. This is shown in Fig. 6 by a single-electron angular distribution calculation as projected for a distance of 150 mm from the source. The two horizontal lobes have different peak intensities and shapes while the vertical OTR lobes are symmetric in intensity and shape as seen in Figs. 6b and 6d. This is particularly true at low gamma (29) as indicated by these calculations. The actual beam divergence has not been convolved, but it is more than 100 times smaller than the OTR pattern's opening angle in our case. Further modeling to explore the observed beam-size polarization effect is warranted.

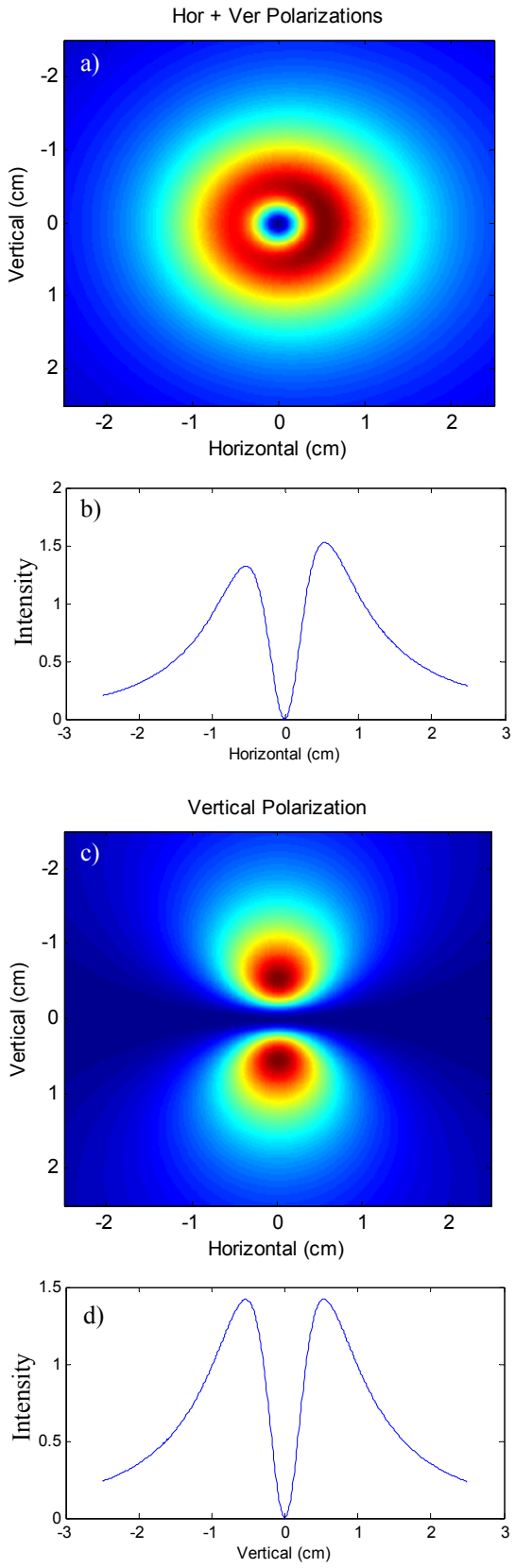

Figure 6: Calculated OTR angular distribution patterns at 150 mm from the source: a) total intensity (sum of both polarizations) b) horizontal profile c) vertically polarized component, and d) vertical profile.

SUMMARY

In summary, we have extended the investigations on OTR polarization effects in beam-size monitoring to the low-gamma regime of the A0PI. We have observed a 20-µm reduction for beam sizes around 100 µm when using the correct polarized component, and we noted this as comparable to the high-gamma results [7]. Due to its nature, we have interpreted it as a term outside of the quadrature treatment for other observed beam size effects and treated it separately. The magnitude of the correction for the slit images is in the 15-20% regime, so corrections are indeed warranted in making emittance calculations. Further modeling of the effect would enhance the understanding of the observations to date.

ACKNOWLEDGEMENTS

The authors acknowledge support from M. Wendt, H. Edwards, E. Harms, and M. Church of Fermilab.

REFERENCES

[1] T. Koeth, L. Bellantoni, D. Edwards, H. Edwards, R. P. Fliller III, "A TM110 Cavity for Longitudinal to Transverse Emittance Exchange", PAC 07, THPAS079, Albuquerque , NM , USA http://www.JACoW.org.

[2] Timothy W. Koeth et al., "Emittance Exchange at the Fermilab A0 Photo Injector", Proc. of PAC09, May 4-8, 2009, Vancouver, B.C., JACoW.

[3] E. Bravin, "Transverse Beam Profiles", Proceedings of Beam Diagnostics CERN Accelerator School, 377-406, CERN-2009-005, and references therein.

[4] C.H. Wang et al., "Slits Measurement of Emittance on TTF", International Conference on Accelerator and Large Experimental Physics Control Systems, Trieste, Italy (1999).

[5] M. Hogan, (private communication, SLAC), May 2005.

[6] A. H. Lumpkin et al., "Initial Imaging of 7-GeV Electron Beams with OTR/ODR Techniques at the APS", Proc. of PAC05, Knoxville, Tenn., p.4162. (2005), http://www.JACoW.org.

[7] Pavel Evtushenko et al., "Near-Field ODR Measurements at CEBAF" , Proc. of BIW08, Lake Tahoe, CA, p.332, (2008), http://www.JACoW.org.

[8] M. Castellano and V.A.Verzilov, Phys. Rev. ST Accel. Beams, 1:062801 (1998).

[9] L. Lyons, Statistics for Nuclear and Particle Physicists (1986).

[10] A.H. Lumpkin et al., "Spatial Resolution Limits of YAG:Ce Powder Beam-profile Monitors at the Fermilab A0 Photoinjector", Proceedings of FEL09, Liverpool, p.348, (2009), http://www.JACoW.org.

[11] K.Floettmann of DESY provided the powder screens which are described in R. Spesyvtsev's Master's Thesis,"Transverse Beam Size Measurement Systems at Photo Injector Test Facility in Zeuthen", (2007).